Available online at www.sciencedirect.com
SCIENCE DIRECT
Trans. Nonferrous Met. Soc. China 17(2007) 138−142
Transactions of Nonferrous Metals Society of China
www.csu.edu.cn/ysxb/

Effects of milling and crystallization conditions on microstructure of $Nd_2Fe_{14}B/\alpha$-Fe powder

WANG Ying(王 迎), WANG Er-de(王尔德)

School of Materials Science and Engineering, Harbin Institute of Technology, Harbin 150001, China

Received 28 March 2006; accepted 17 October 2006

Abstract: Effects of milling and crystallization conditions on microstructure, such as amorphous phase and nanocrystalline phase, were investigated by X-ray diffractometry(XRD), differential scanning calorimetry(DSC), and transmission electron microscopy (TEM), respectively. The results show that nanocomposite $Nd_2Fe_{14}B/\alpha$-Fe powder can be prepared by mechanical milling in argon atmosphere and a subsequent vacuum annealing treatment. The grain sizes of both $Nd_2Fe_{14}B$ and α-Fe phase decrease drastically with increasing milling time. After milling for 5 h, the as-milled material consists of α-Fe nanocomposite phases with the grain size of 10 nm, and some amorphous phases, which can be turned into $Nd_2Fe_{14}B/\alpha$-Fe nanocomposite phases by the subsequent annealing treatment. Milling energy of mechanical milling after 5 h by theoretical calculation is 6 154.25 kJ/g.

Key words: mechanical milling; crystallization treatment; $Nd_2Fe_{14}B/\alpha$-Fe; grain size; milling energy

1 Introduction

In recent years, considerable attention has been focused on nanocomposite $Nd_2Fe_{14}B/\alpha$-Fe magnets[1−4], because they have remanences J_r larger than the Stoner-Wohlfarth value $J_s/2$ (J_s, saturation magnetic polarization) and can maintain high coercivity. The nanocomposite magnets are composed of a hard phase ($Nd_2Fe_{14}B$) and a soft phase (α-Fe). Among the nanometer grains (＜100 nm), exchange coupling exists, leading to a reduced remanence J_r/J_s of about 0.7 and to a higher Curie temperature. But the values of the maximum energy product $(BH)_{max}$ achieved experimentally have been much smaller than those predicted theoretically[5−8].

As we know, the microstructure of $Nd_2Fe_{14}B/\alpha$-Fe plays an important role in magnetic properties. Much effort has been made to optimize microstructure by using various preparation methods, such as mechanical alloying, melt spinning or sputtering, and element substitution. Mechanical milling as an alternative preparation technique to produce nano-structured Nd-Fe-B powder has also been reported by many authors[9−12]. Mechanical milling has a unique advantage of refining microstructure of powder materials, and it can lead to an amorphous or nanocrystalline alloy powder that must be subsequently annealed to restore the $Nd_2Fe_{14}B$ hard magnetic phase.

In this paper, the effects of milling and crystallization conditions on the microstructure, such as amorphous phase and nanocrystalline phase, were investigated.

2 Experimental

The starting materials were the as-cast $Nd_2Fe_{14}B$ alloy with total impurities less than 0.5% (mass fraction) and carbonylic iron powder with total impurities less than 0.1% (mass fraction). The powder mixtures were milled in an attritor ball mill under a purified argon atmosphere for 5 h. The mass ratio of ball to powder was 20:1 and the milling rotation speed was 300 r/min. The as-milled powder was heat-treated at various temperatures for 30 min in vacuum sintering furnace.

For the purpose of preventing oxidation, the charging and discharging of the alloy powder were performed in a glove box. Before milling operation, the vial was evacuated and then filled with argon until the pressure of 0.1 MPa was reached. This procedure was repeated whenever subsequent discharging operation was carried out to take sample powder out from the mill. The

Corresponding author: WANG Ying; Tel: +86-451-86414267; E-mail: wangying1002@hit.edu.cn

phase changes due to ball milling and subsequent heat treatment were characterized by X-ray diffraction(XRD) using Cu K_α radiation. Particle sizes of alloy powder were measured with an atom force microscope(AFM), a transmission electron microscope (TEM) and scanning electron microscope(SEM). Differential scanning calorimetry(DSC) was employed to determine the crystallization temperature of alloy powder. The effect of milling energy on amorphous phase and nanocrystalline phase formed was investigated.

3 Results and discussion

3.1 Effect of milling time on microstructure

Fig.1 shows the XRD patterns of the alloy powder milled for various time in argon atmosphere. It was seen that the starting powder (denoted by 0 h in Fig.1) was characterized by a dominant tetragonal $Nd_2Fe_{14}B$ phase, i.e., the magnetic matrix of the NdFeB alloy, and a portion of free α-Fe. By mechanical milling in argon, the diffraction peaks of both $Nd_2Fe_{14}B$ and α-Fe phase became gradually broadened in width and decreased in intensity. However, no new peaks were observed. This suggests that mechanical milling in argon does not change the constituent phases, $Nd_2Fe_{14}B$ and α-Fe, of the alloy, but the crystallite sizes of $Nd_2Fe_{14}B$ and α-Fe phase decrease steadily with increasing milling time. After 5 h milling, the alloy powders have decomposed into an amorphous phase and nanocrystalline α-Fe phase.

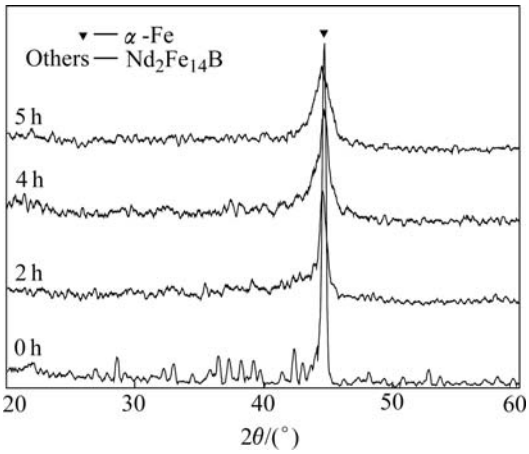

Fig.1 XRD patterns of alloy powder milled for various time

The average grain sizes of $Nd_2Fe_{14}B$ phase and α-Fe phase for various milling time were estimated by X-ray diffraction using Scherrer's formula $D=0.9\lambda/(B\cos\theta)$[13], as listed in Table 1.

Obviously, the grain size of $Nd_2Fe_{14}B$ and α-Fe phase was decreased apparently with increasing the milling time. After 2 h, the grain sizes of $Nd_2Fe_{14}B$ and α-Fe phase were 40 nm and 31 nm respectively. After 5 h milling, the as-milled material consisted of α-Fe nano-composite phase with grain size of 10 nm, and some amorphous phase.

Table 1 Effect of milling time on grain size

Milling time/h	Grain size of $Nd_2Fe_{14}B$ phase/nm	Grain size of α-Fe phase/nm
2	40	31
4	20	15
5	Amorphous	10

TEM image and corresponding electron diffraction pattern of alloy powder milled for 5 h in argon atmosphere are shown in Fig.2. The TEM observations and electron diffraction patterns show that the alloy powder milled in argon atmosphere for 5 h consists of amorphous phase and nanocrystalline α-Fe phase with a grain size of about 10 nm, which is consistent with the XRD results.

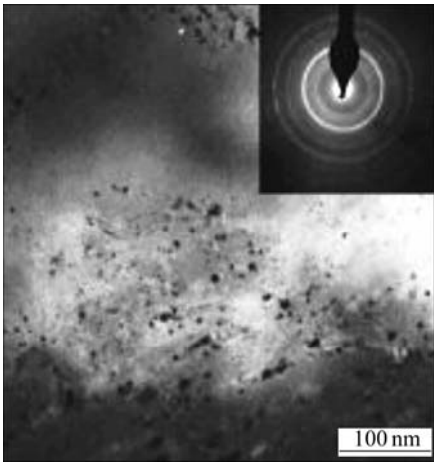

Fig.2 TEM image and corresponding electron diffraction pattern of alloy powder milled for 5 h

Figs.3(a), (b) and (c) show the particle size of alloy powder for various milling time. It is obvious that the particle size of the powder decreases with increasing milling time. Agglomerated particle is observed evidently in Fig.3, which causes difficulty in measuring the particle size exactly.

In order to observe particle size and particle distribution of powder, AFM analysis result is shown in Fig.4. It can be seen that particle distribution of powder was uniform and the average particle size was 0.2−0.3 μm after milling for 5 h. Both the small particle size and uniform structure are beneficial to obtaining the optimum microstructure after heat-treatment.

3.2 Effect of crystallization temperature on micro-structure

In order to determinate the crystallization temperature accurately, DSC analysis result of alloy powder milled for 5 h is shown in Fig.5. It is obvious that

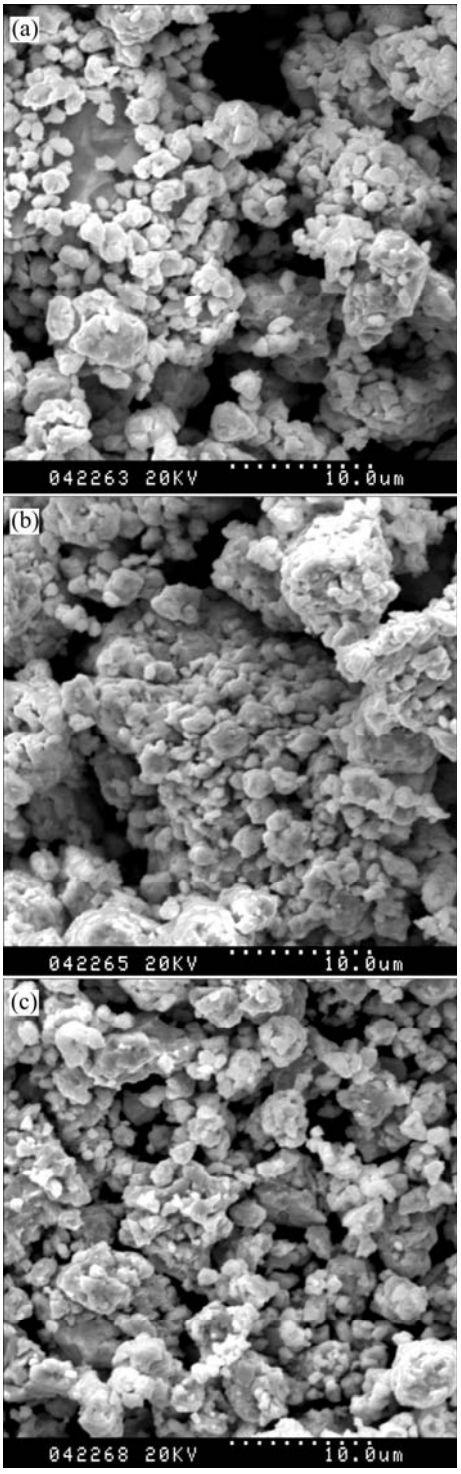

Fig.3 SEM images of alloy powder milled for various time: (a) 2 h; (b) 4 h; (c) 5 h

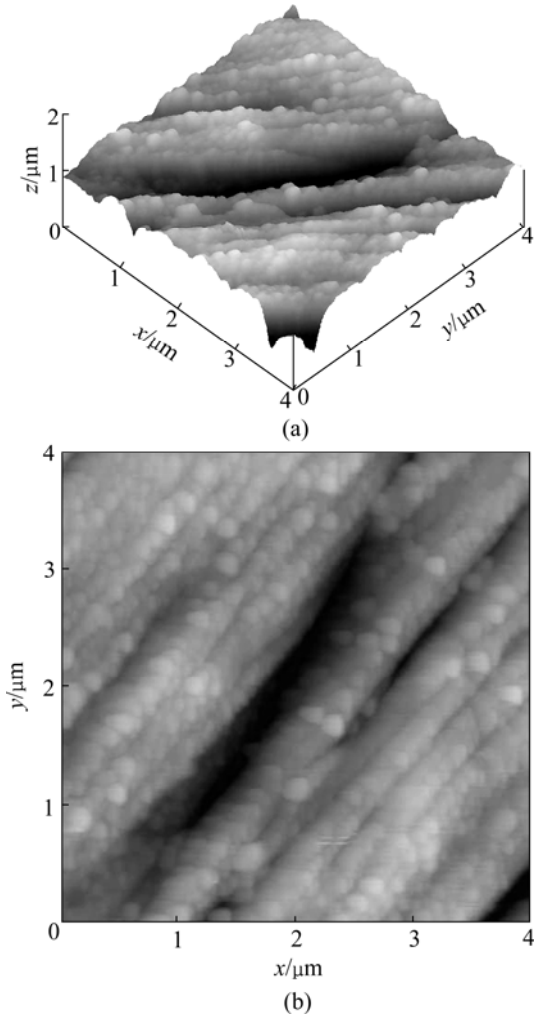

Fig.4 AFM images of alloy powder milled for 5 h: (a) 3D-pattern; (b) 2D-pattern

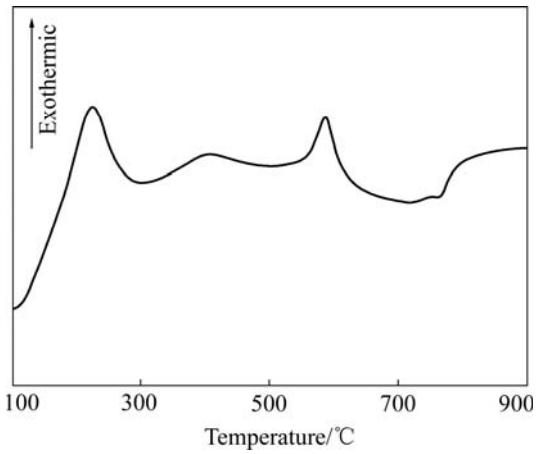

Fig.5 DSC analysis results of alloy powder milled for 5 h

there are three exothermic peaks in Fig.5. The first exothermic peak that occurred near 230 ℃ was caused by strain energy during milling. Crystallization temperature of α-Fe was 440 ℃ [14], which corresponded to the second peak in Fig.5. $Nd_2Fe_{14}B$ phase was crystallized between 600 ℃ and 800 ℃. Based on the DSC analysis, crystallization temperature of alloy powder was chosen as 650, 700 and 750 ℃ for 30 min milling, respectively.

Fig.6 shows that nanocrystalline $Nd_2Fe_{14}B$ phase coexisted of α-Fe in nanoscale. Moreover, $Nd_2Fe_{14}B$ phase crystallized completely at 650 ℃ for 30 min. The diffraction peaks of $Nd_2Fe_{14}B$ and α-Fe phase became gradually narrowed in width and increased in intensity.

This suggests that the grain size of $Nd_2Fe_{14}B$ and α-Fe phase increases steadily with increasing crystallization temperature. It means that it is not necessary to enhance crystallization temperature further.

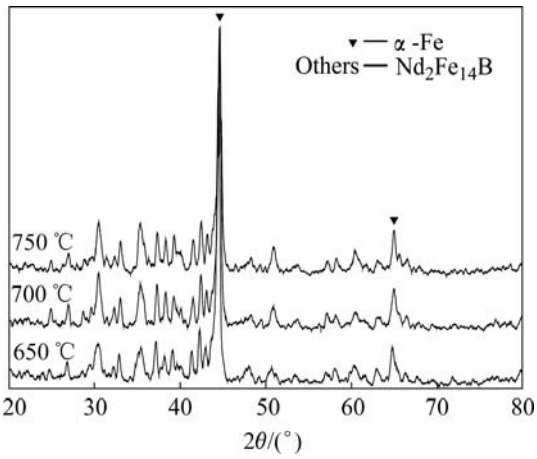

Fig.6 XRD patterns of alloy powder for various crystallization temperatures

Variation in grain size of $Nd_2Fe_{14}B$ and α-Fe phase with different crystallization temperatures is listed in Table 2. In general, increase of grain size due to increasing crystallization temperature was observed. The grain sizes of $Nd_2Fe_{14}B$ phase and α-Fe phase were 30 nm and 41 nm at 650 ℃. Furthermore, grain growth rate of α-Fe phase was larger than that of $Nd_2Fe_{14}B$.

Table 2 Grain size of alloy powder for various crystallization temperatures

Crystallization temperature/℃	Grain size of $Nd_2Fe_{14}B$/nm	Grain size of α-Fe/nm
650	30	41
700	52	65
750	70	90

TEM micrograph of alloy powder crystallized at 650 ℃ for 30 min is shown in Fig.7. It is obvious that $Nd_2Fe_{14}B$ phase was crystallized from amorphous phase. Grain size of $Nd_2Fe_{14}B$ phase was about 30 nm and grain size of α-Fe phase was about 40 nm, which was consistent with the results of Table 2 based on XRD patterns. The $Nd_2Fe_{14}B$/α-Fe powder with fine grain size will build good foundation on obtaining permanent magnetic materials with high properties.

3.3 Calculation of milling energy

Based on the calculation model[15], plastic deformation energy of powder can be written as

$$E_t = \frac{N_b}{2} \cdot n_c \cdot E_p \quad (1)$$

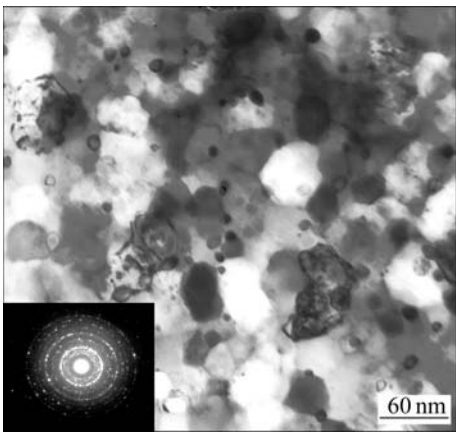

Fig.7 TEM micrograph of alloy powder crystallized at 650 ℃ for 30 min

where N_b is ball number and n_c is number of collision.

E_p is plastic deformation energy of the powder at each collision, which can be written as

$$E_p = \int_0^{\varepsilon_{max}} V_c \cdot \sigma_s \cdot d\varepsilon = V_c \cdot \sigma_s \cdot \varepsilon_{max} \quad (2)$$

where V_c is volume of the powder caught by each collision and σ_s is flow stress of powder.

ε_{max} is strain of the powder after each collision, which can be given by

$$\varepsilon_{max} = \ln(\frac{h_0}{h_1}) \quad (3)$$

where h_0 is height of powder before collision and h_1 is height after collision.

According to Eqn.(1) and milling parameter, the calculated milling energy is listed in Table 3. The milling energy of attritor ball milling reached 6 154.25 kJ/g after milling for 5 h. While for planetary ball milling it was 1 204.1 kJ/g after milling for 30 h[16], which demonstrated that the efficiency of attritor ball milling was higher than that of planetary ball milling.

Table 3 Attritor ball milling enegy with different milling time

σ_s/ MPa	V_c/ ($10^{-6}m^3$)	L_f/ m	V/ ($m \cdot s^{-1}$)	E_t/($kJ \cdot g^{-1}$)		
				2 h	4 h	5 h
2	9.4	0.076	1.5	2 461.70	4 923.40	6 154.25

4 Conclusions

1) After milling for 5 h, the as-milled materials are composed of amorphous and α-Fe nanocomposite phase with grain size of about 10 nm. The particle sizes of the alloy powder milled for 5 h is about 0.2−0.3 μm. The distribution of particles is uniform.

2) Alloy powder after milling for 5 h is crystallized

at different temperatures. The grain sizes of $Nd_2Fe_{14}B$ and the α-Fe phase are 30 nm and 41 nm at 650 ℃, respectively. Furthermore, grain growth rate of α-Fe phase is larger than that of $Nd_2Fe_{14}B$ phase.

3) The calculated milling energy of attritor ball milling reaches 6 154.25 kJ/g after 5 h milling, which is the sextuple of that of planetary ball milling after 30 h milling. It demonstrates that the efficiency of attritor ball milling is higher than that of planetary ball milling.

References

[1] KNELLER E F, HAWIG R. The exchange-spring magnet: A new material principle for permanent [J]. IEEE Trans on Mag, 1991, 27: 3588−3600.

[2] RYBALKA S B, DODONAVA E V, DIDUS V A. Some kinetic and microstructural aspects during hydrogen-induced phase transformations in $Nd_2Fe_{14}B$ alloys [J]. J Alloys Compounds, 2005, 404−406: 588−594.

[3] HAN G B, GAO R W, YAN S S, LIU H Q, FU S, FENG W C, LI W, LI X M. Effect of exchange-coupling interaction on the effective anisotropy in nanocrystalline $Nd_2Fe_{14}B$ material [J]. J Magn Magn Mater, 2004, 281: 6−10.

[4] SCHREFL T, FIDLER J, KRONMÜLLER H. Remanence and coercivity in isotropic nanocrystalline permanent magnets [J]. Phys Rev B, 1994, 49: 6100−6110.

[5] MADAAH-HOSSEINI H R, KIANVASH A. The role of milling atmosphere on microstructure and magnetic properties of a $Nd_{12.8}Fe_{79.8}B_{7.4}$-type sintered magnet [J]. J Magn Magn Mater, 2004, 281: 92−96.

[6] GUTFLEISCH O, BOLLERO A, HANDSTEIN A, HINA D, KIRCHNER A. Nanocrystalline high performance permanent magnets [J]. J Magn Magn Mater, 2002, 242/245: 1277−1283.

[7] SKOMSKI R, COEY J M D. Giant energy product in nanostructured two phase magnets [J]. Phys Rev B, 1993, 48: 15812−15816.

[8] SSHEN B G, ZHANG H W, ZHANG W Y, YAN A R. Synthesis and magnetic properties of nanocrystalline rare-earth permanent magnetic materials [J]. Journal of the Chinese Rare Earth Society, 2004, 22(1): 28−33. (in Chinese).

[9] XIAO Q F, ZHAO T, ZHANG Z D, BRUCK E, BUSHOW K H J, DE BOER F R. Effect of grain size and magntocrystalline anisotropy on exchange coupling in nanocomposite two-phase Nd-Fe-B magnets [J]. J Magn Magn Mater, 2001, 223(3): 215−220.

[10] SHADROV V G, NEMTSEVICH L V. Nanocrystalline magnetic materials [J]. Fizika I Khimiya Obrabotki Materialov, 2002, 5: 50−61.

[11] MCCORMICK P G, MIAO W F, DING J, STREET R. Remanence-enhanced $Nd_8Fe_{87}M_1B_4$ (M=Fe, V, Si, Ga, Cr) alloys [J]. J Magn Magn Mater, 1998, 177/181: 976−977.

[12] LIU W, ZHANG Z D, SUN S K, HE J F, TANG H, Cui B Z, ZHAO X G. Effect of nitrogen content on structure and magnetic properties of $Nd_{16}Fe_{84-x}B_xN_y$ alloys prepared by mechanical alloying [J]. J Alloys Compounds, 2000, 309: 172−175.

[13] SHENG S X. X-ray Diffraction Analysis [M]. Beijing: Metallurgical Industry Press, 1986. 441. (in Chinese)

[14] ZHANG M, ZHANG Z D, SUN X K, LIU W, GENG D Y, JIN X M, YOU C Y, ZHAO X G. Remanent enhancement of nanocomposite $(Nd, Sm)_2Fe_{14}B/\alpha$-Fe magnets [J]. J Alloys Compounds, 2004, 372: 267−271.

[15] LIANG Guo-xian. Research on the Formation of Binary Amorphous Alloy by Mechanical Alloying [D]. Harbin: Harbin Institute of Technology, 1992: 32−60. (in Chinese)

[16] SHI Gang. Preparation of Nanocrystalline $Nd_2Fe_{14}B/\alpha$-Fe Permanent Magnetic Material by Mechanical Milling-HDDR Processing [D]. Harbin: Harbin Institute of Technology, 2005: 28−90 (in Chinese)

(Edited by YANG Bing)